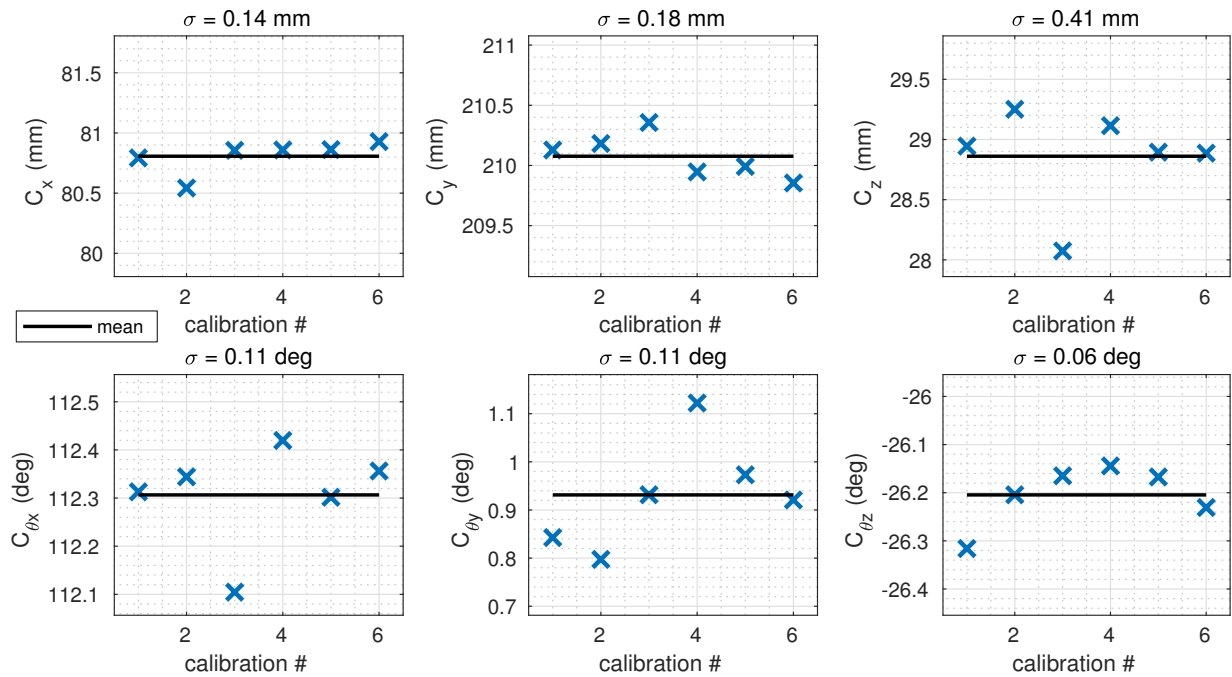
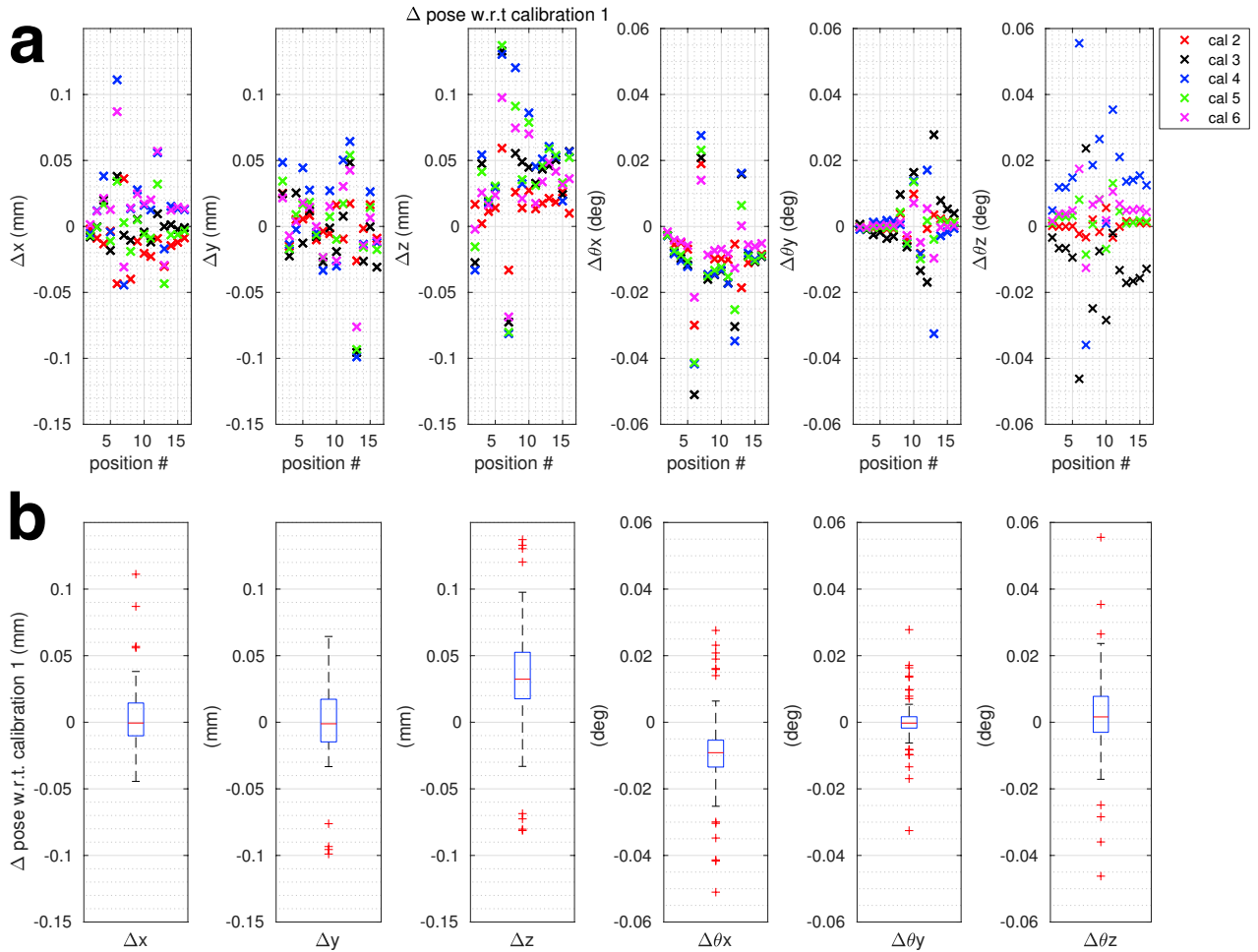


Supporting Information Video S1: Time lapse video of the point clouds recorded during an *in-vivo* discrete motion experiment with T2-SPACE PMC. The first half of the video corresponds to the motion during the within ET PMC scan, and the second half corresponds to the scan without PMC.

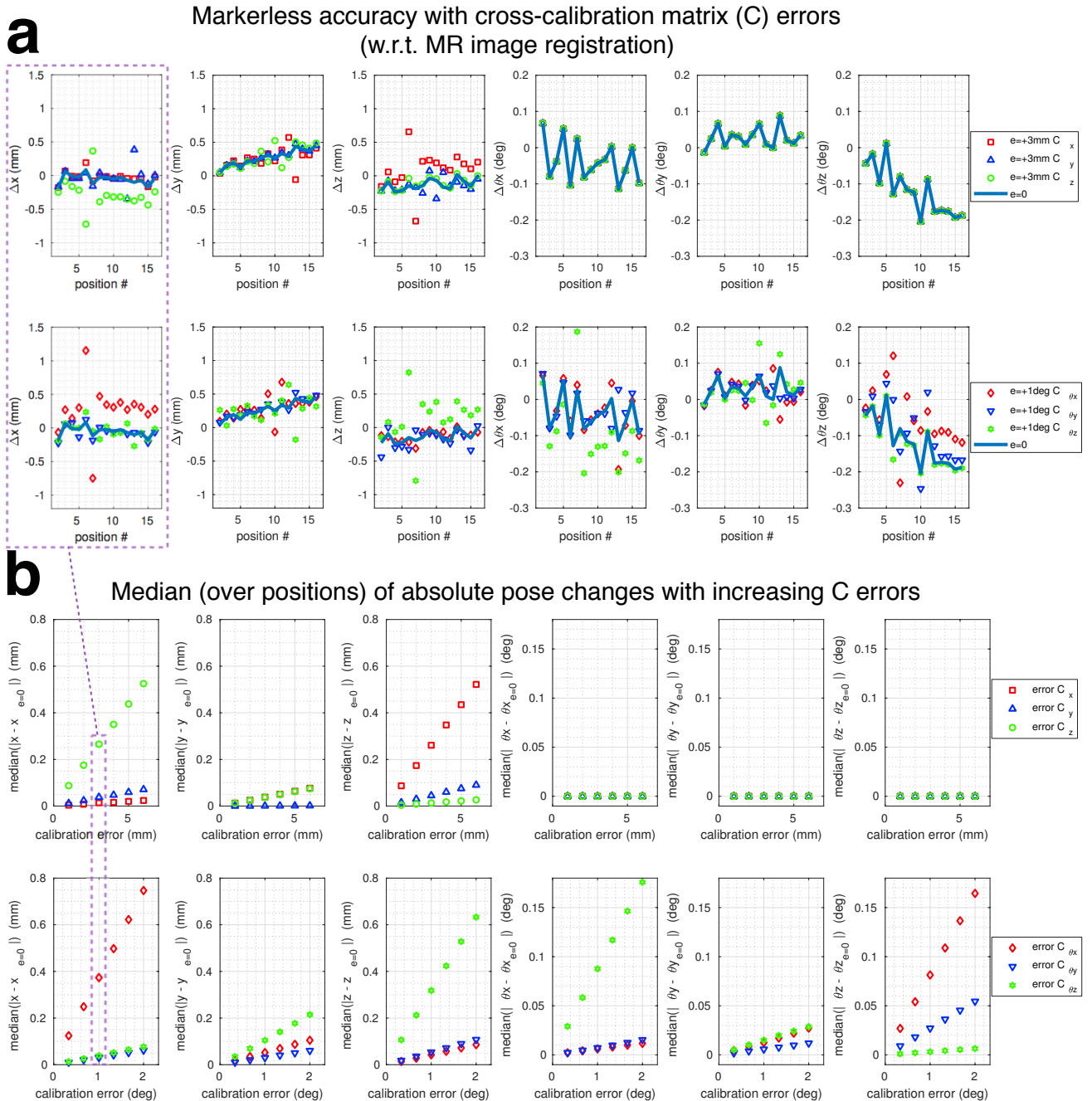
Supporting Information Video S2: Time lapse video of point clouds showing the deviations in pose estimates associated with: eyes open versus closed; blinking; frowning; looking left versus right. The video shows the experiment where the subject's eyes were not cropped.



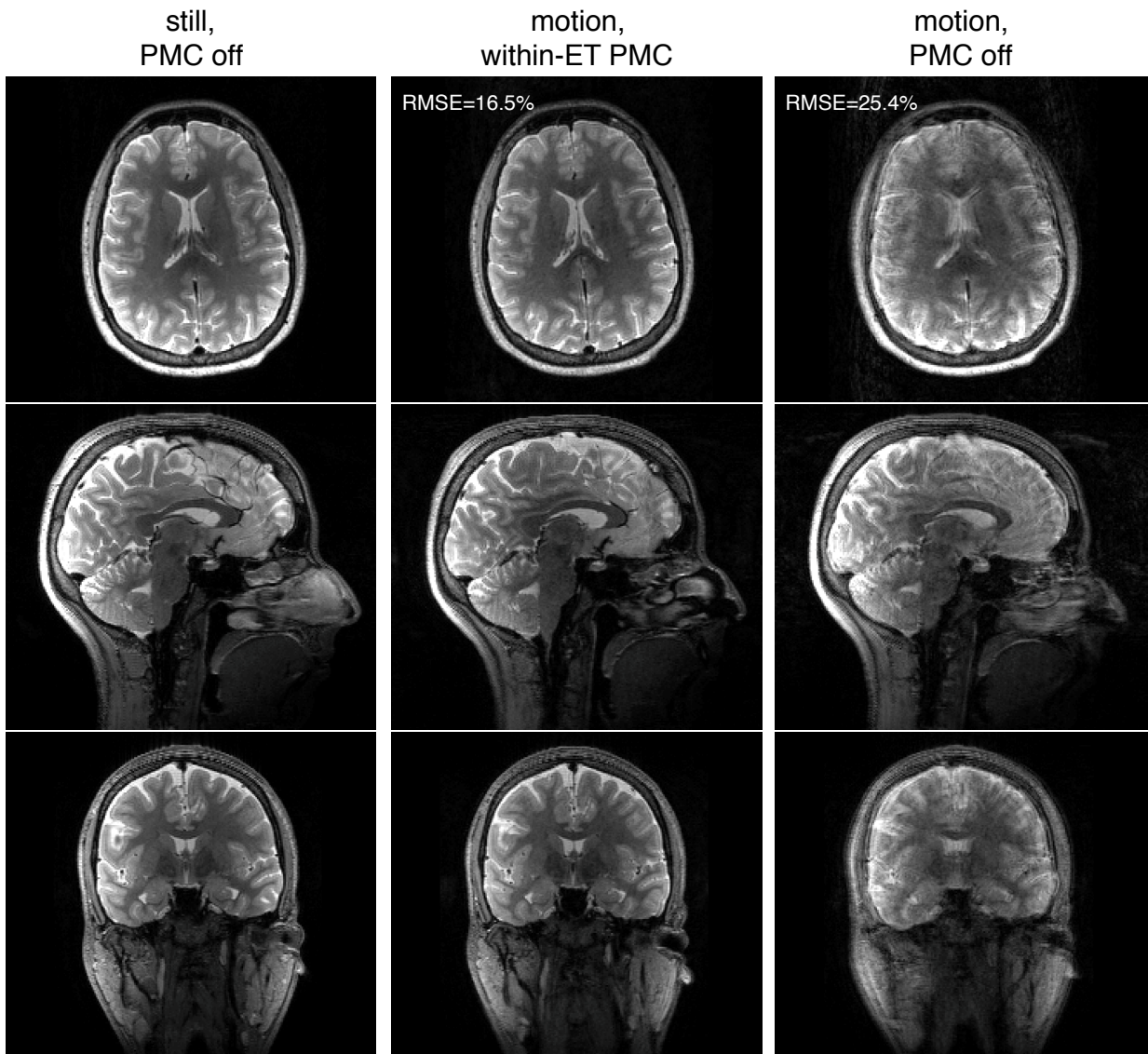
Supporting Information Figure S1: The rigid body parameters from 6 repeated cross-calibrations with a phantom. The phantom was moved to different positions for each of the 6 calibrations.



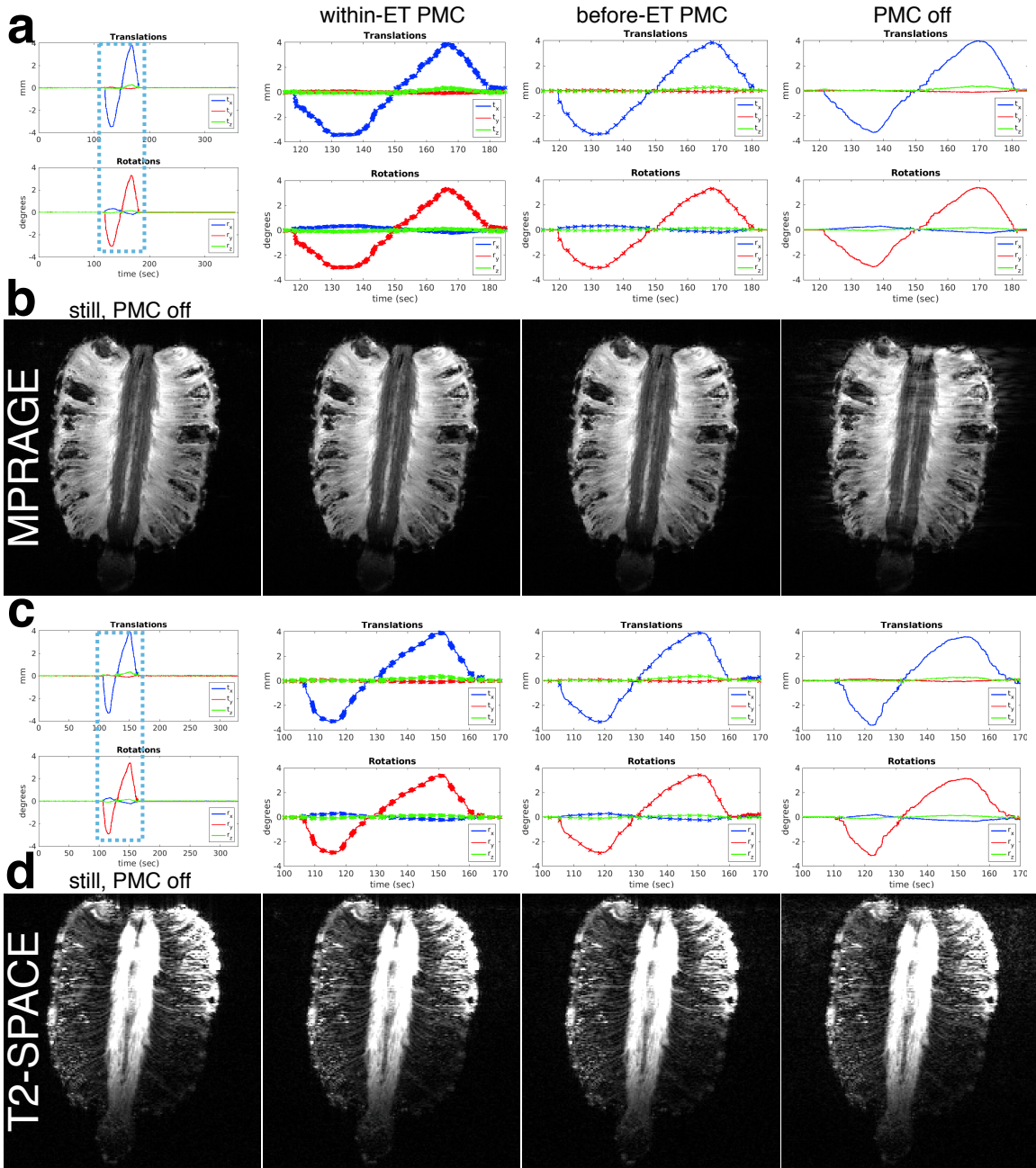
Supporting Information Figure S2: Estimation of pose variability introduced by surface matching cross-calibration. The tracking accuracy data with 15 movements from position 1 was used to compute pose estimates from six repeated calibrations. (a) The change in pose between the first calibration and the subsequent five calibrations, for all 15 movements. (b) The median pose changes over all calibrations and all movements.



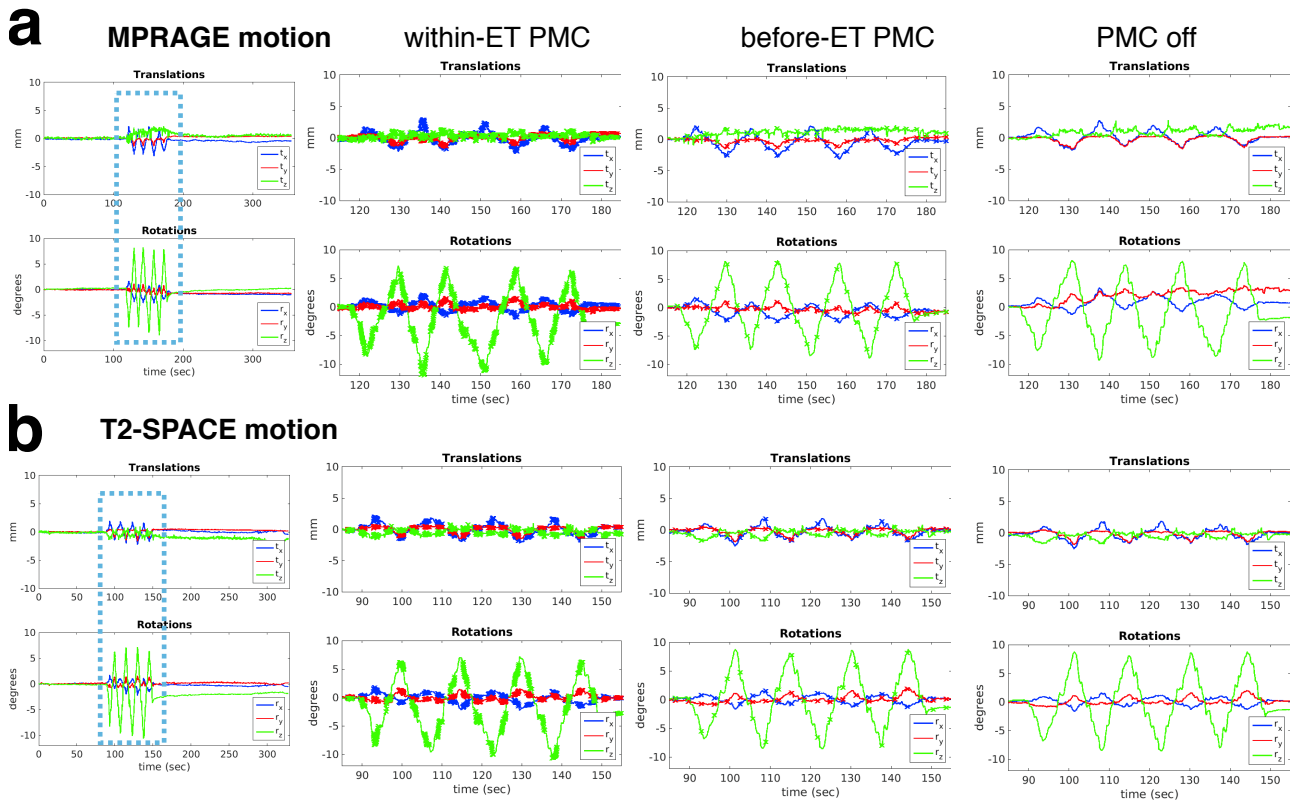
Supporting Information Figure S3: Changes in pose estimates induced by cross-calibration errors. (a) Pose estimates in the accuracy experiment with 3 mm (top row) and 1° changes (bottom row) in the rigid body parameters of the cross-calibration matrix. The thick blue line shows the original data from the accuracy experiment with the measured calibration matrix (zero error). (b) Median absolute pose changes for varying calibration errors relative to the measured calibration. The dotted purple box shows the correspondence for the x translation pose estimates with 3 mm and 1° errors, and the median summaries of absolute changes over all positions.



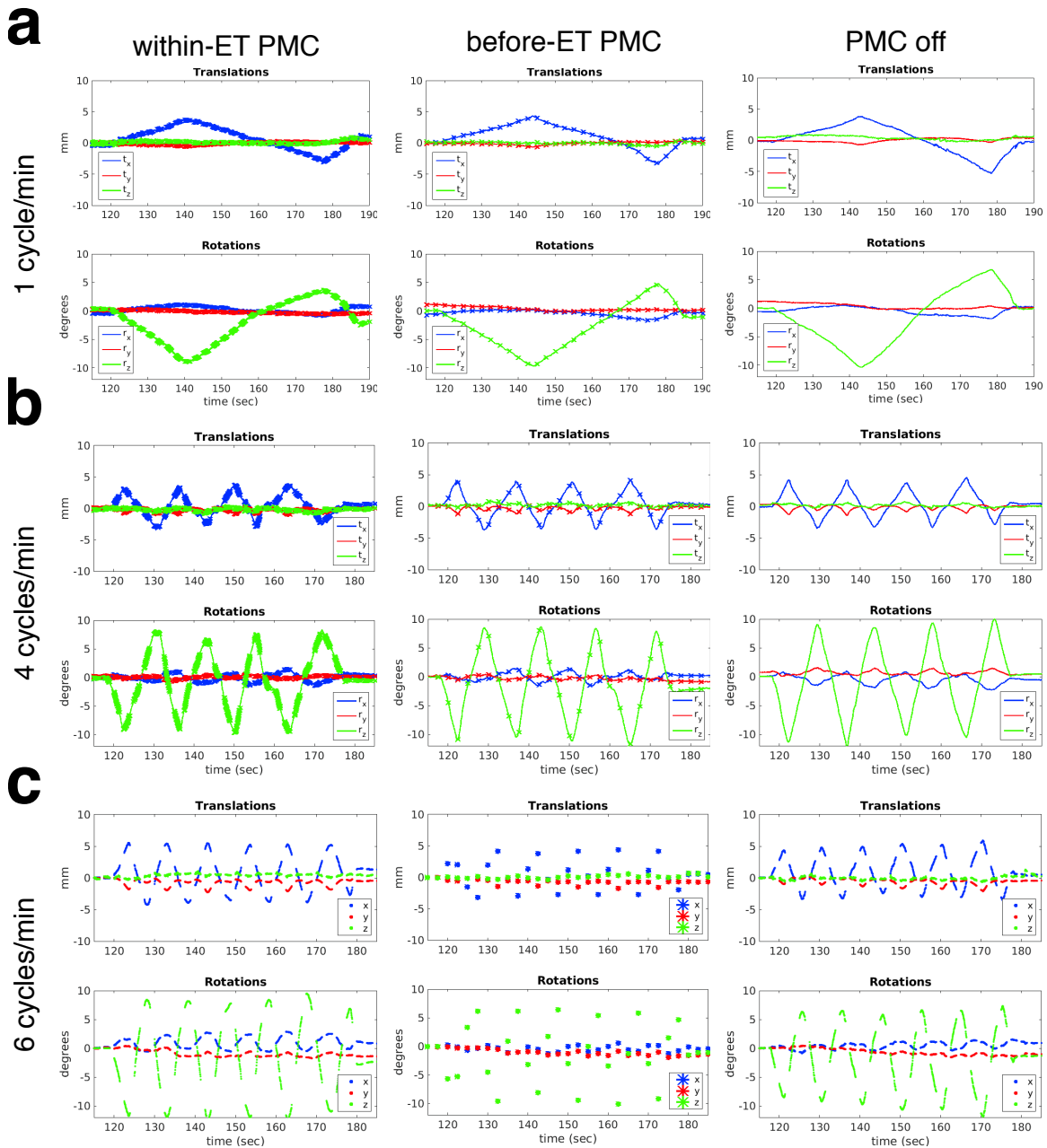
Supporting Information Figure S4: *In vivo* comparison of images acquired during the discrete motion shown in Supporting Video S1 using within ET PMC (middle column) and no PMC (right), and a still scan (left) for reference.



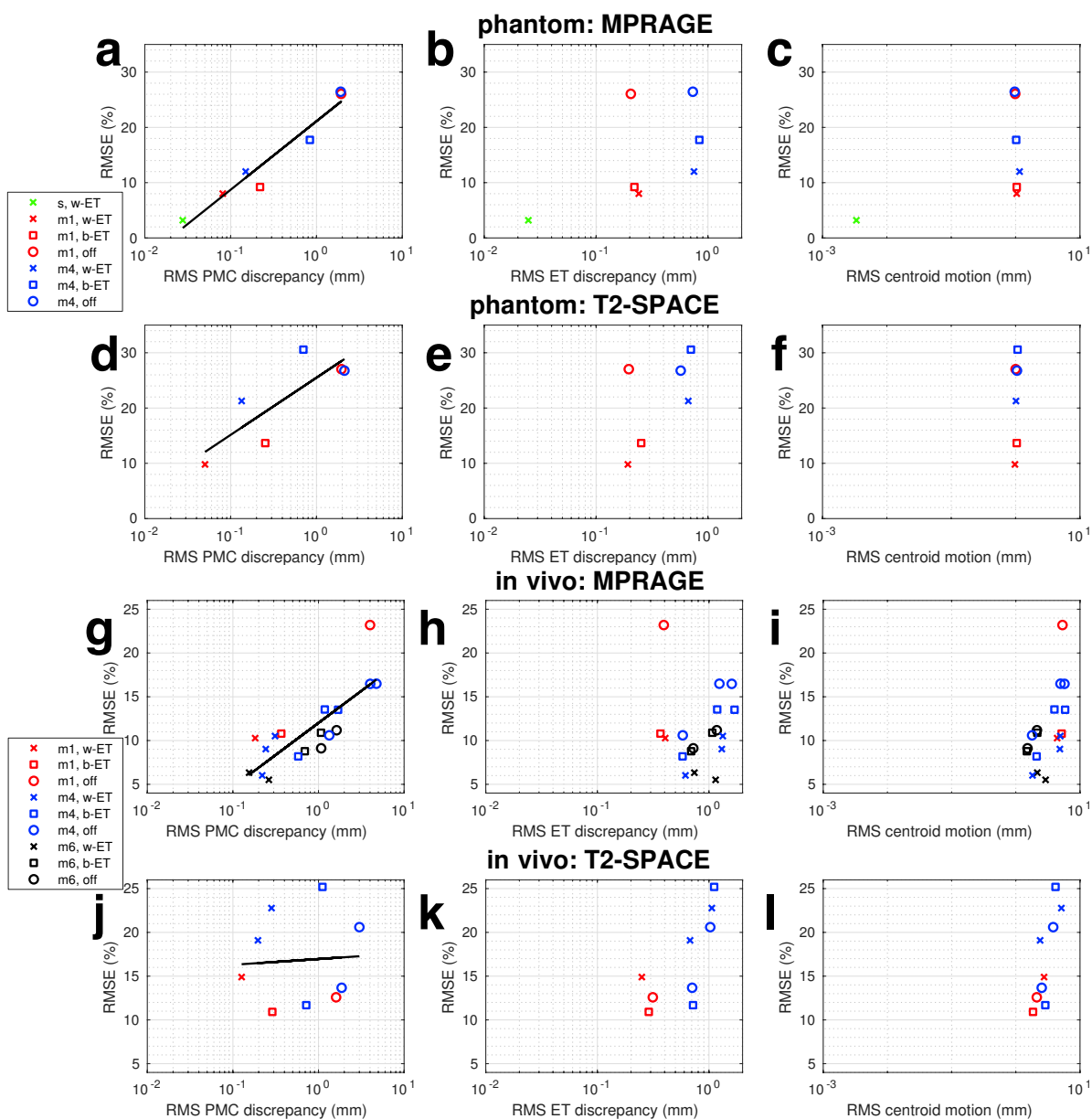
Supporting Information Figure S5: Phantom comparison of PMC off, before-ET PMC, and within-ET PMC image quality during 1 cycle/min continuous motion. Zoomed plots of the changes to the FOV position and orientation during the three separate MPRAGE (a) and T2-SPACE (c) motion scans. Crosses on the plots represent updates to the encoded FOV. MPRAGE (b) and T2-SPACE (d) image quality of a reference scan without motion and the three motions scans with different PMC. Images are windowed to highlight ghosting artefacts.



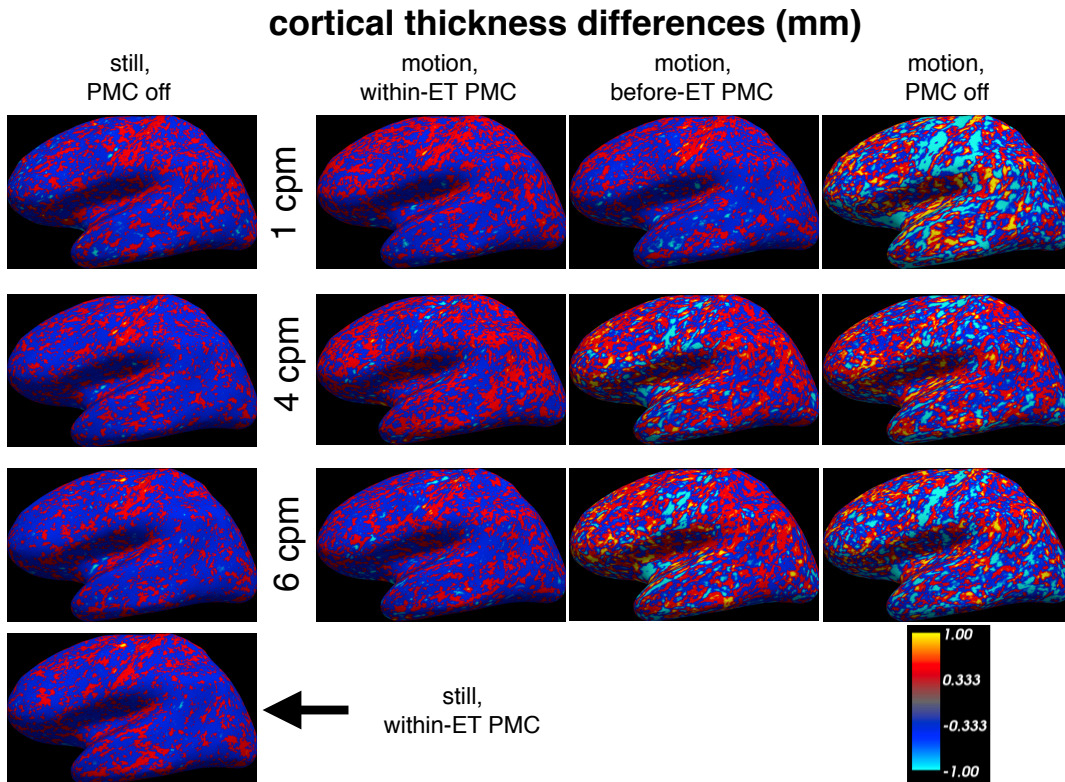
Supporting Information Figure S6: Motion information for the *in vivo* (a) MPRAGE and (b) T2-SPACE experiments with 4 cycle/min continuous motion with subject 2. The zoomed plots show changes to the FOV position and orientation during the motion periods of each scan. Crosses on the plots represent updates to the encoded FOV.



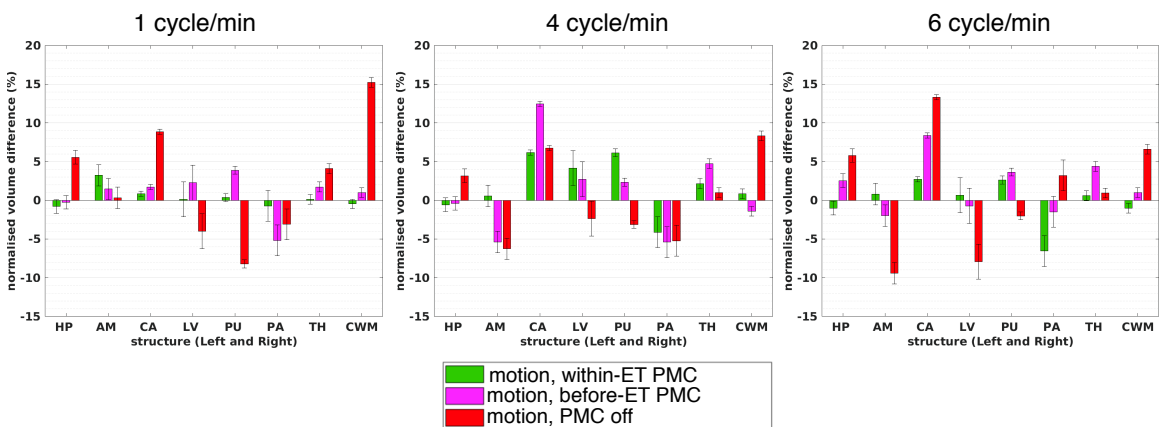
Supporting Information Figure S7: Motion information for the *in vivo* MPRAGE experiment with 1, 4, and 6 cycle/min continuous motion with subject 3. Each row shows zoomed plots of the changes to the FOV position and orientation (pose) during the three separate motion scans for each motion speed. Crosses on the plots represent updates to the encoded FOV. Note that in the 6 cycle/min experiment (c) the complete motion information was not available due to technical problems, and only the updates sent to the scanner were stored. In scans with PMC off, updates were sent to the scanner and recorded to allow for the possibility of retrospective motion, but they were not used to update the FOV pose in real-time.



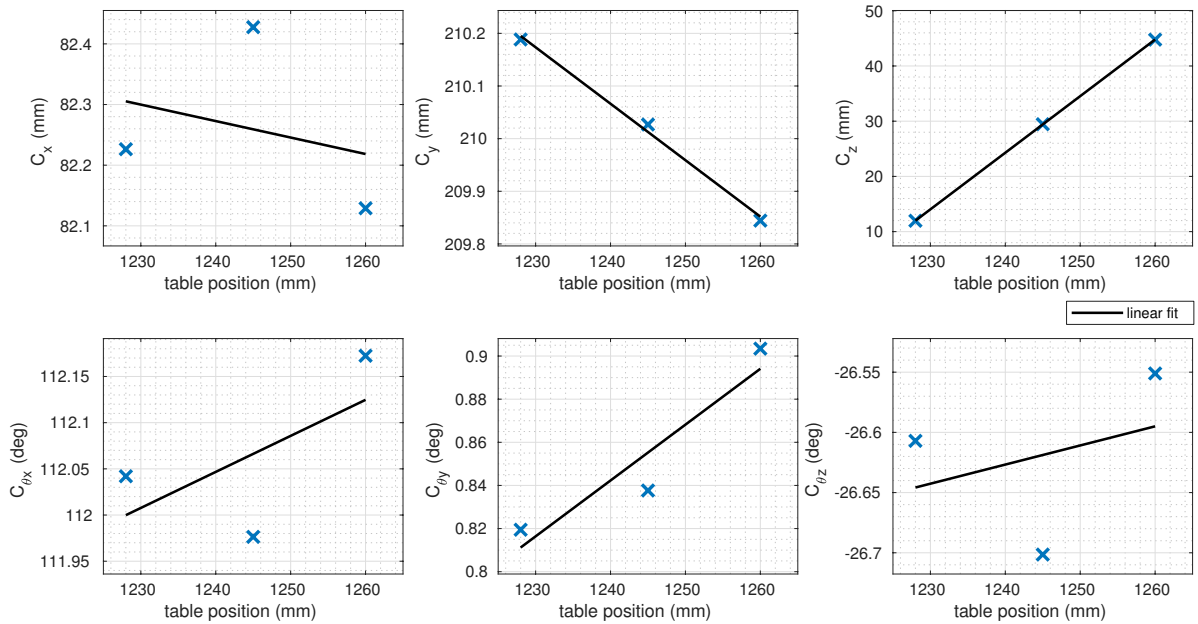
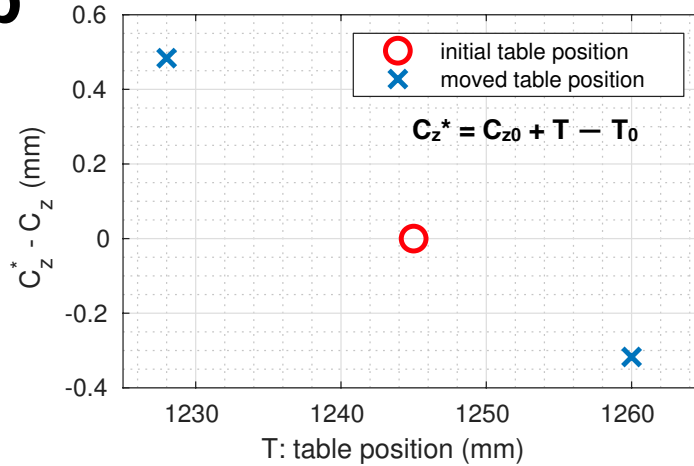
Supporting Information Figure S8: Comparisons of image quality measured by normalised RMSE (relative to a still scan without intentional motion) versus RMS PMC discrepancy (left column), RMS ET discrepancy (middle column), and RMS centroid motion (right column). Data from experiments with 1, 4, and 6 cycle/min motion are shown in red, blue, and black, respectively. Note that the full motion information was not recorded for the 6 cycle/min session with subject 3 so the motion summaries could not be generated. Key for scan labels: s=still; m1=motion, 1 cycle/min; m4=motion, 4 cycle/min; m6=motion, 6 cycle/min; w-ET=within-ET PMC; b-ET=before-ET PMC; off=PMC off.



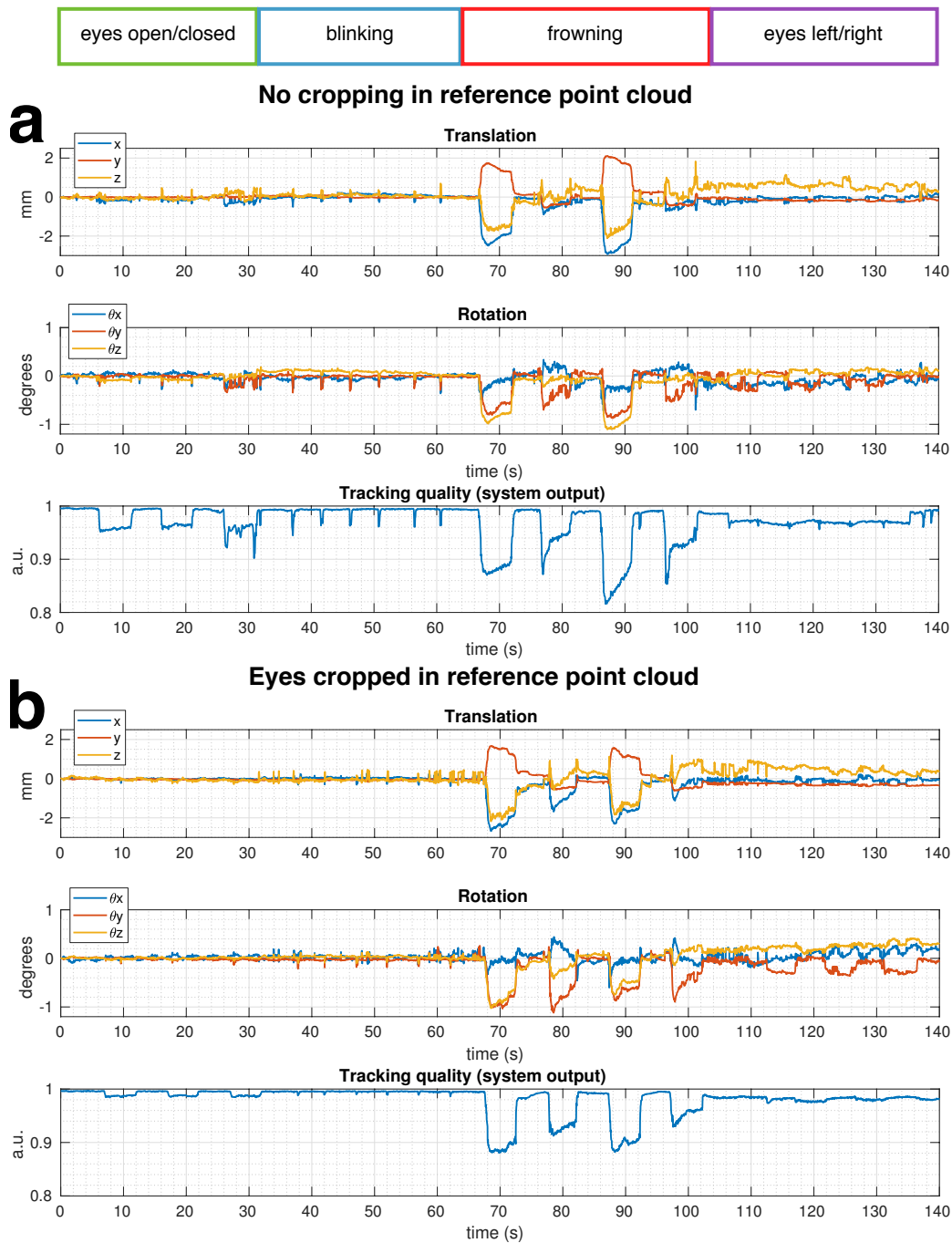
Supporting Information Figure S9: Unsmoothed cortical thickness differences in mm from the robust median surface for all of the 13 scans acquired with subject 3.



Supporting Information Figure S10: Comparison of subject 3's brain structure volumes estimated from MPRAGE scans acquired during 1, 4, and 6 cycle/min of continuous motion. Normalised volume differences from the gold standard (mean of four "still" scans) are shown for PMC off, before-ET PMC and within-ET PMC. Key for brain structures: HP=hippocampus; AM=amygdala; CA=caudate; LV=lateral ventricles; PU=putamen; PA=pallidum; TH=thalamus; CWM=cerebral white matter.

a**Variation of calibration parameters with table position****b****Table-position-corrected (C_z^*) vs measured (C_z)**

Supporting Information Figure S11: Assessment of table position correction for the cross-calibration matrix. (a) The rigid body parameters from 3 cross-calibration matrices when the table was moved from an initial position (1245 mm) to 2 different positions. The change in parameters is small (less than 0.3 mm and 0.1°), except for the z translation entry C_z , which is the table movement dimension. (b) Comparison of two table-corrected C_z^* values to measured C_z . The C_z^* values were computed by accounting for the difference in reported table position as shown in the equation on the graph. Differences are comparable with the intrinsic variability of the calibration estimated in the repeated calibration experiment (see Supporting Information Fig. S1).



Supporting Information Figure S12: Pose deviations associated with eye movement and frowning and comparison of (a) no cropping in the reference point cloud versus (b) cropping the eyes. The eye movement or frowning test conditions are indicated at the top of the Figure. The tracking system provides a “quality” parameter, which could potentially be used to detect abrupt point cloud shape deviations from the reference point cloud. See Supporting Information Video S2 for the point clouds acquired during the experiment shown in Fig. S12a.